mater.scichina.com link.springer.com

Published online 11 June 2020 | https://doi.org/10.1007/s40843-020-1327-8
Sci China Mater 2020, 63(9): 1683–1692

Large-scale synthesis of lithium- and manganese-rich materials with uniform thin-film Al_2O_3 coating for stable cathode cycling

Yuqiong Kang[1,2†], Zheng Liang[5†], Yun Zhao[3,4*], Haiping Xu[4], Kun Qian[4], Xiangming He[3], Tao Li[4*] and Jiangang Li[1,2*]

ABSTRACT **The lithium- and manganese-rich layered oxide (LMR) holds great promise as a cathode material for lithium-ion battery (LIB) applications due to its high capacity, high voltage and low cost. Unfortunately, its poor initial Coulombic efficiency (ICE) and unstable electrode/electrolyte interface with continuous growth of the solid electrolyte interphase leads to high impedance and large overpotential. These effects cause severe capacity loss and safety issues. In this work, we have developed a novel approach to fabricate a stable LMR cathode with a uniform thin layer of aluminum oxide (Al_2O_3) coated on the surface of the LMR particles. This synthesis approach uses the microemulsion method that is environment-friendly, cost-effective and can be easily scaled. Typically, an 8-nm layer of Al_2O_3 is shown to be effective in stabilizing the electrode/electrolyte interface (enhanced ICE to 82.0% and moderate impedance increase over 200 cycles). Moreover, the phase transformation from layered to spinel is inhibited (96.3% average voltage retention) and thermal stability of the structure is significantly increased (heat release reduced by 72.4%). This study opens up a new avenue to address interface issues in LIB cathodes and prompts the practical applications of high capacity and voltage materials for high energy density batteries.**

Keywords: lithium ion batteries, lithium- and manganese-rich layered oxides, surface modification, metal oxide thin film, uniform coating, large-scale synthesis, battery safety

INTRODUCTION

The development of energy storage systems is an essential component in energy and environmental sciences [1]. Compared with numerous energy storage devices such as nickel-metal hydride and lead-acid batteries, lithium-ion batteries (LIBs) have attracted wide attention due to the high energy density, high cell voltage, long cycle life, and wide operating temperature range [2]. The energy density of a full cell is determined by both the cathode and anode materials. With recent progress in anode materials with high capacities, the energy density of LIBs is now limited by the cathode materials (~150 mA h g^{-1}) [3,4]. As a result, focus has turned to develop cathode materials with high potential and high specific capacity [5,6]. The conventional cathode materials that have dominated the battery market for over 30 years [7], including the layered $LiCoO_2$ (working voltage 3.7 V, 150 mA h g^{-1}), spinel $LiMn_2O_4$ (3.7 V, 120 mA h g^{-1}) and olivine $LiFePO_4$ (3.2 V, 140 mA h g^{-1}), fail to meet the demand of energy densities above 300 W h kg^{-1}. Therefore, it is important to develop next-generation cathode materials with specific capacities ≥200 mA h g^{-1} and voltages above 4 V [8]. The materials $LiNi_xMn_yCo_zO_2$ (NMC*xyz*, 3.7 V, ~200 mA h g^{-1} according to Ni content) [9,10], Li-rich layered oxides (4.2 V, 280 mA h g^{-1}) [11], and $LiNi_{0.5}Mn_{1.5}O_4$ (LNM, 4.7 V, 147 mA h g^{-1}) [12] are a few of the candidate cathode materials that approach these desirable capacities and voltages.

Among the cathode materials, lithium- and manganese-rich $Li_{1+x}M_{1-x}O_2$ (LMR) has high capacity and voltage, which has attracted intensive interest [13,14]. However, the practical application of LMR is limited by the fol-

[1] School of Chemical Engineering, Beijing Institute of Petrochemical Technology, Beijing 102617, China
[2] Beijing Key Laboratory of Fuels Cleaning and Advanced Catalytic Emission Reduction Technology, Beijing 102617, China
[3] State Key Laboratory of Automotive Safety and Energy, Tsinghua University, Beijing 100084, China
[4] Department of Chemistry and Biochemistry, Northern Illinois University, DeKalb, IL 60115, USA
[5] Materials Sciences Division, Lawrence Berkeley National Laboratory, Berkeley, CA 94720, USA
† These authors contributed equally to this work.
* Corresponding authors (emails: yzhao.zjut@hotmail.com (Zhao Y); tli4@niu.edu (Li T); lijiangang@bipt.edu.cn (Li J))

lowing issues [15–22]: (1) the carbonate electrolyte usually decomposes at voltages above 4.3 V *vs.* Li/Li^+, exacerbating the electrode-electrolyte side reactions. These reactions create a thick solid electrolyte interphase (SEI) layer accompanied by the generation of heat and gases, the consumption of lithium sources, and increased impedance; (2) the loss of lithium from the Li_2MnO_3 phase lowers the initial Coulombic efficiency (ICE) [15]; (3) the metastable transition metal phase of the LMR surface results in irreversible Li deintercalation [16], and a gradual phase transformation from the surface to the interior of the material, leading to severe capacity and voltage fade [17]; (4) the oxygen generated from the phase transformation is consumed by the battery [21], causing the sharp increase of temperature and swelling of the cell, which leads to possible thermal runaway and safety issues [22].

It is well accepted that the practical application of LMR is mainly hindered by interface issues. Strategies such as surface coating, elemental doping and morphology control, are generally used to address the above issues. Directly coating on the interface is an effective way to suppress the interfacial reactions [23–31]. A number of approaches, such as spray pyrolysis [32], sol-gel method [33], and vapor deposition method [34], have been employed to inhibit the electrolyte decomposition. However, it is still challenging to achieve a controlled uniform coating at nanoscale. The atomic layer deposition (ALD) is the only method that produces controlled nanoscale thin films; however, the high-cost of precursors, as well as the slow deposition rates make this approach only applicable in the laboratory-scale [35]. Therefore, a scalable environment-friendly and cost-effective method for uniform coating at a large scale is needed.

Herein, we proposed a microemulsion-based coating strategy using solutions of alkaline metal ions to prepare a uniform thin layer of metal oxide in a large-scale, environment-friendly and economical way (Fig. 1). Since the surface of the LMR is alkaline and polar, it will be rapidly covered with metal-ions (Al^{3+}, Mg^{2+}, Ba^{2+}, etc.) homogeneously when immersed in an alkaline metal ion solution. These uniformly dispersed metal-ions will interact with the surface of the LMR to form a pre-coating layer. This layer is very stable due to the strong physical and chemical interactions and can be converted into the corresponding metal oxide layer when exposed in air. To demonstrate the viability of this concept, Al_2O_3 coating was selected as an example based on the following considerations: (1) while Al_2O_3 is a typical isolating material to protect the electrode surface from electrolytes and acids [36], it is also an electronic and ionic insulator. When adopted as the protective layer for electrodes, the thickness of the Al_2O_3 coating should be precisely controlled as small fluctuation dramatically changes electronic and ionic conductivities [37]. (2) LMR is a water-sensitive material, so coatings should avoid the use of any aqueous solutions. (3) For a green and economical process, the solvents should be recyclable and reusable for practical applications at large-scale.

This method enables surface modification of LMR ($Li_{1.2}Ni_{0.2}Mn_{0.6}O_2$) and NMC622 with high quality and large quantities (20 g per batch in the laboratory). All the

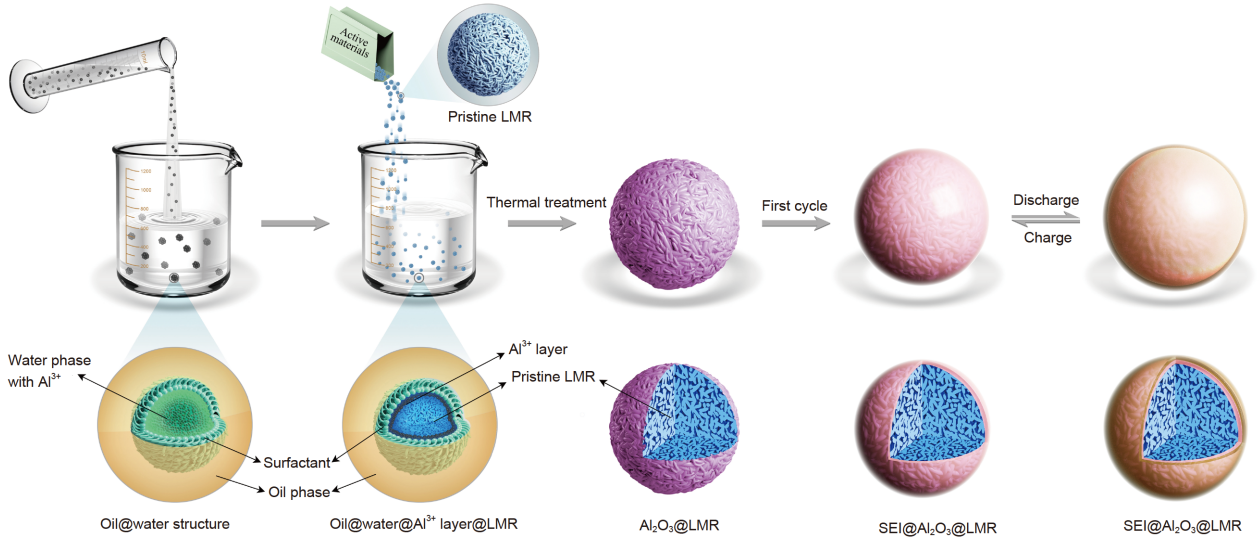

Figure 1 Schematic diagrams of the entire coating process on the surface of LMR material and the function of this Al_2O_3 coating during charge-discharge cycles.

solvents in the process can be recycled and reused. We investigated the effects of fabrication conditions on the electrochemical performance and optimized the stoichiometric ratio of the solvents in the microemulsion. Long-term cycling performance, impedance characterization, and thermal stability analysis demonstrate that the modified LMR can stabilize the surface and bulk structure during cycling. Specifically, the exothermic temperature of the modified LMR from safety tests increased from 255 to 273°C and the heat release was reduced by 72.4%.

EXPERIMENTAL SECTION

Materials

$NiSO_4{\cdot}6H_2O$ and $MnSO_4{\cdot}H_2O$ were purchased from Tianjin Fuchen Co. Ltd. (China). NaOH and TritonX-100 were purchased from Xilong Scientific Co. Ltd. (China). $Al(NO_3)_3{\cdot}9H_2O$, 1-methyl-2-pyrrolidinone (NMP), *n*-hexanol and cyclohexane were purchased from Sinopharm Chemical Reagent Beijing Co. Ltd. (China). Li metal, Li_2CO_3, acetone and ammonia solution (25 wt% in water) were purchased from Beijing Chemical Works (China). Carbon black, separator Celgard2400 and polyvinylidene fluoride (PVDF) were purchased from Guangdong Canrd New Energy Technology Co., Ltd. (China). All of the materials were used without further purification.

Synthesis of LMR

The pristine LMR was prepared by co-precipitation with $NiSO_4{\cdot}6H_2O$ and $MnSO_4{\cdot}H_2O$ as the precursor, NaOH as the precipitant, and $NH_3{\cdot}H_2O$ as the complexing agent. The pH value, temperature and stirring speed were precisely controlled to be 11.5, 55°C and 550 r min^{-1}, respectively. Afterwards, the obtained materials were dried in a vacuum oven at 120°C for 12 h. The as-prepared $Ni_{0.2}Mn_{0.6}(OH)_{1.6}$ was then mixed with a proportion of Li_2CO_3. The mixture was calcined at 500°C for 6 h, and then heated to 850°C for 12 h at air atmosphere to obtain pristine LMR materials.

Synthesis of the Al_2O_3-coated LMR

TritonX-100 (surfactant) was mixed with *n*-hexanol (co-surfactant) with a ratio of 3:2 by weight. Then 100 g of the as-prepared mixture was mixed with 500 mL of cyclohexane (oil phase) at room temperature. After magnetic stirring for 20 min, 7.5 mL of an Al^{3+} solution (aqueous phase) with a certain concentration was added into the oil solution, and the mixture was ultrasonically emulsified for 30 min to obtain a clear and transparent microemulsion. Afterwards, 0.25 mol of LMR material was added to the above microemulsion, stirred for 5 h at 80°C to remove the oil phase. Finally, the obtained materials were rinsed with acetone, vacuum dried at 120°C and then placed in a furnace at 500°C for 6 h to fabricate the Al_2O_3-coated LMR (labeled as Al_2O_3-0.2%, Al_2O_3-0.5%, Al_2O_3-1.0% and Al_2O_3-2.0% according to different molar ratios of Al^{3+} to LMR).

Characterizations

The morphology, structure and elemental distribution of the samples were examined by field emission scanning electron microscopy (FE-SEM, Hitachi SU-8010, Japan), transmission electron microscopy (TEM, Hitachi JEM-2100, Japan), and energy dispersive spectrometer (EDS). The X-ray diffraction (XRD, Shimadzu XRD-7000, Japan) was used to analyze the crystal structure of the LMR. Dynamic light scattering (DLS, Wyatt DynaPro NanoStar, USA) was used to measure the size of the water phase in the microemulsion. The thermal stability of the material was tested by differential scanning calorimeter (DSC, American TA Instruments SDT Q600).

Electrochemical measurements

The electrochemical performance was evaluated using coin cells with LMR and Li foil as the positive and negative electrodes, respectively. The positive electrodes were prepared by mixing LMR, conductive carbon black and binder (PVDF) with a mass ratio of 8:1:1 in NMP to form an uniform slurry. The slurry was uniformly coated on the aluminum foil and dried in a vacuum oven at 120°C for more than 12 h (mass loading about 4.2 mg cm^{-2}). The electrolyte employed was 1 mol L^{-1} $LiPF_6$ in a mixture of ethylene carbonate, dimethyl carbonate and ethyl methyl carbonate ($v/v/v$=1:1:1). The galvanostatic cyclability and rate capability (1 C=250 mA h g^{-1}) were examined on a Land system (LAND-CT2001A, BTRBTS) in the voltage range of 2.0–4.8 V. Electrochemical impedance spectra (EIS, 1 MHz–0.01 Hz) were measured using an IM-6ex electrochemical workstation.

RESULTS AND DISCUSSION

Synthesis and characterization of the Al_2O_3-coated LMR materials

The microemulsion method was applied to modify the precursor materials in large quantity. An aqueous solution containing Al^{3+} (aqueous phase, acidic and polar) was added to the oil phase to form an oil@water struc-

ture. The Al^{3+} were dispersed in the aqueous phase droplets (Fig. 1). Due to the basicity and polarity of the LMR surface, the aqueous phase favorably covered the surface of the LMR uniformly when the LMR was dispersed in the microemulsion. The $Al(OH)_3$ was converted into a uniform coating of Al_2O_3 when the modified LMR was exposed in air (Fig. 1). In this process, the microemulsion provided an environment for the homogeneous distribution of Al^{3+} on the surface of LMR. The surfactant, cosurfactant and oil phase remained unchanged before and after the process and could be recycled based on their different boiling points (TritonX-100 (270°C), *n*-hexanol (157°C), cyclohexane (80°C)). The recycled solvents can be used again after drying with anhydrous sodium sulphate.

The water content has a significant influence on the coating. With high water content, excess water reacted with the surface of LMR, while the microemulsion phase was damaged when the water content was too low. The thickness of the coating was mainly determined by the Al^{3+} concentration. Low Al^{3+} concentration lead to poor coverage of LMR while high Al^{3+} concentration and the large droplet microemulsion caused agglomeration of Al_2O_3 and low coating quality. The optimal oil to water ratio was 200:3 in volume, and we optimized the Al^{3+} concentration with this ratio. Fig. 2a shows the diameter distribution of water droplets at different Al^{3+} concentrations. In the microemulsion, the water droplet size is correlated with Al^{3+} concentration. It is speculated that the thickness of Al_2O_3 coating on the LMR surface will correlate with the Al^{3+} concentration. Effective surface modification of LMR not only stabilizes the interface but can also positively influence the battery cycle life, rate behavior, voltage hysteresis, impedance, and safety.

The XRD patterns of the Al_2O_3-modified LMR with different coating thicknesses are shown in Fig. 2b. All the peaks index the hexagonal structure of α-$NaFeO_2$, except for the weak diffraction peaks in the range of 2θ=20°–22°, and the space group symmetry is *R*3*m*. The adjacent peaks of (006)/(012) and (108)/(110) are clearly separated, indicating that the samples have a highly ordered layered structure. The weak peak between 20° and 22° shows a monoclinic Li_2MnO_3 phase, and the space group symmetry is *C*2/*m*, indicating the short-range ordered structure of Li-Mn cations in the transition metal layer. The XRD patterns before and after coating are consistent, and no additional Al_2O_3 diffraction peaks are observed, which may be attributed to the amorphous nature of the Al_2O_3 thin-film. After fitting, it is found that the unit cell parameters (*a* and *c*) of the materials increased slightly with the coating thickness. This change may be ascribed to the partial transformation of the amorphous Al_2O_3 into Li_xAlO_2, which is caused by the reaction of nano-Al_2O_3 layer and trace amount of Li_2O at the surface of LMR during the thermal treatment to form a fast Li^+ conductor [38,39]. Overall, there is no significant change in the lattice parameters of all the samples, and the values of $I_{(003)}/I_{(104)}$ and $I_{(006)}+I_{(012)}/I_{(101)}$ ($I_{(xxx)}$ represents the diffraction intensity of the *xxx* peak in XRD patterns) have no obvious changes, indicating that the Al_2O_3 coating has minimal effects on the internal structure of LMR particles.

To further study the microstructure of the LMR surface and confirm the presence of Al_2O_3, SEM and TEM were used to characterize the pristine LMR and Al_2O_3-1.0% samples. As seen in Fig. 3a, b, there is no significant distinctions in the overall morphology and structure between the pristine LMR and the Al_2O_3-1.0%, except for minor morphology changes on the surface where the previously clearly-observed primary particles become blurred after coating. The Al_2O_3 coating covers the surface of each single particle, and the adjacent primary particles agglomerate with the coating. The distribution of the elements on the LMR surface was further analyzed by EDS analysis. As shown in Fig. 3c and Fig. S1, the surface of LMR is uniformly distributed with O, Al, Mn,

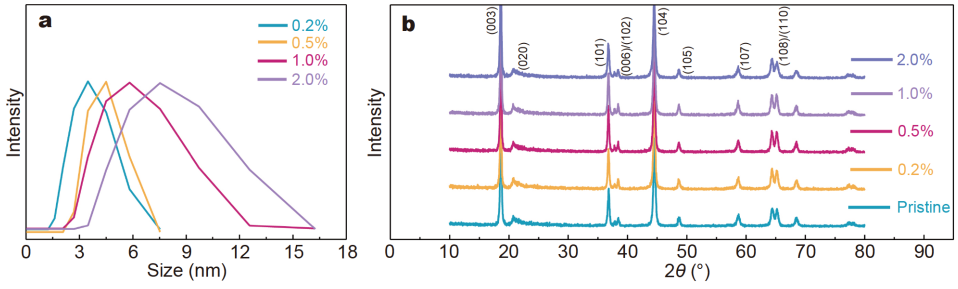

Figure 2 (a) The aqueous droplet diameter distribution with different Al^{3+} concentrations in microemulsion; (b) XRD patterns of the pristine and Al_2O_3-coated LMR.

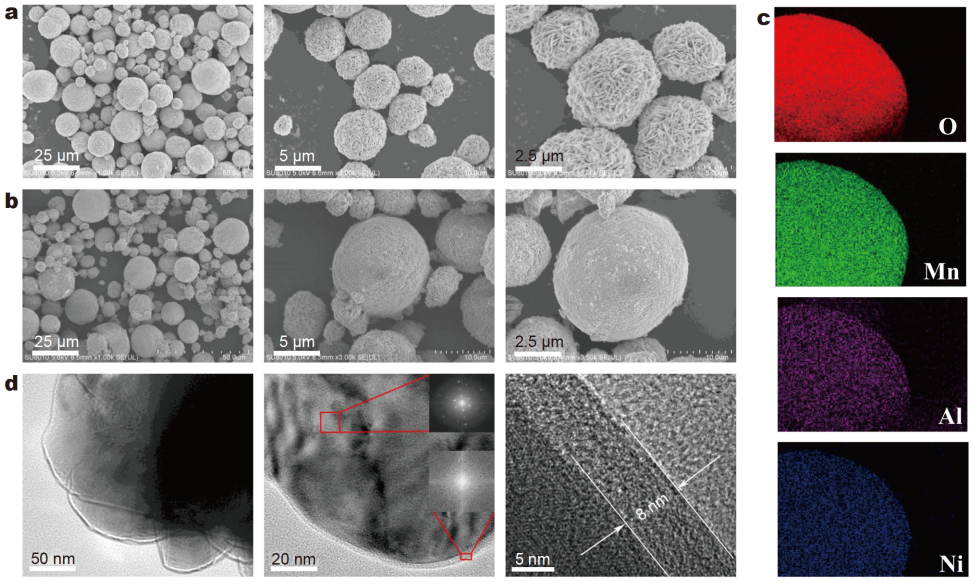

Figure 3 (a) SEM images of the pristine LMR material; (b) SEM images of the Al_2O_3-1.0%; (c) EDS mapping of the O, Mn, Al and Ni elements of the Al_2O_3-1.0%; (d) HRTEM images of Al_2O_3-1.0%.

and Ni. The abundant O and Mn elements are distributed with high-intensity EDS signals. Since the concentration of Al^{3+} used for coating is around 1%, the Al signal exhibits a very weak intensity, as presented in Fig. S1. The high-resolution TEM (HRTEM) was performed to further examine the coating quality. Fig. 3d demonstrates that there is a uniform thin film with a thickness of around 8 nm on the surface of the Al^{3+}-1.0% LMR sample, compared with the uncoated sample (Fig. S2). This evidence supports the successful formation of the Al_2O_3 layer that could increase the stability of the LMR material interface.

Electrochemical performances of the Al_2O_3-coated LMR materials

Electrochemical performances of the surface-modified LMR materials with various Al^{3+} contents were analyzed. Fig. 4a displays that all the samples exhibit similar voltage profiles for the initial galvanostatic cycle, showing a typical LMR cycling characteristics [40]. In comparison with other coating processes using aqueous solutions, no spinel phase appears in this work, which would otherwise decrease the discharge voltage plateau [41,42]. The specific capacities for the charge process decrease from 438.5, 425.3, 429.9 to 411.7 mA h g^{-1} and for the discharge process increase from 312.2, 306.7, 315.5 to 337.5 mA h g^{-1}, respectively, with increasing Al^{3+} content to 1.0% (Table S1). These shifts in capacity mean the ICE rises from 71.2% to 82.0%. The loss in charge capacity but increase in discharge capacity may relate to the suppressed oxygen loss [15], phase transformation [16], and side reactions between the electrode and electrolyte [18] at high charge voltage, indicating the Al_2O_3 coating is able to stabilize the interface and internal structure of the LMR cathode, bringing more stability to SEI formation. However, as the Al^{3+} content reaches 2.0%, the charge and discharge voltage profiles are polarized, owing to the thicker coating and the agglomeration of Al_2O_3 that hinders the transport of electrons and Li^+ ions (Fig. S3). Therefore, with 1.0% Al^{3+} concentration, the modified LMR has the highest reversible capacity, and an initial discharge specific capacity of 337.5 mA h g^{-1}. In the following discussion, focus will be on the modified LMR with 1.0% Al_2O_3 coating. It is worth noting that the recycled solvents from the 1.0% Al^{3+} microemulsion was reused to make a new 1.0% Al_2O_3-coated LMR that demonstrated comparable electrochemical performances with the previously-made samples.

Cycling behavior and rate capability were also investigated. As seen in Fig. 4b, the initial discharge capacity of the pristine LMR is 193.0 mA h g^{-1} at 0.5 C, while the capacities for the modified LMR samples with Al^{3+} concentrations of 0.2%, 0.5%, 1.0% and 2.0% are 192.5, 199.8, 209.2, and 184.4 mA h g^{-1}, respectively. After 50 cycles, the discharge capacity of the pristine LMR material decreases to 182.6 mA h g^{-1} with a retention rate of 94.6%. In contrast, the optimized Al_2O_3-modified sample shows a better cyclability and capacity retention of 97.2%.

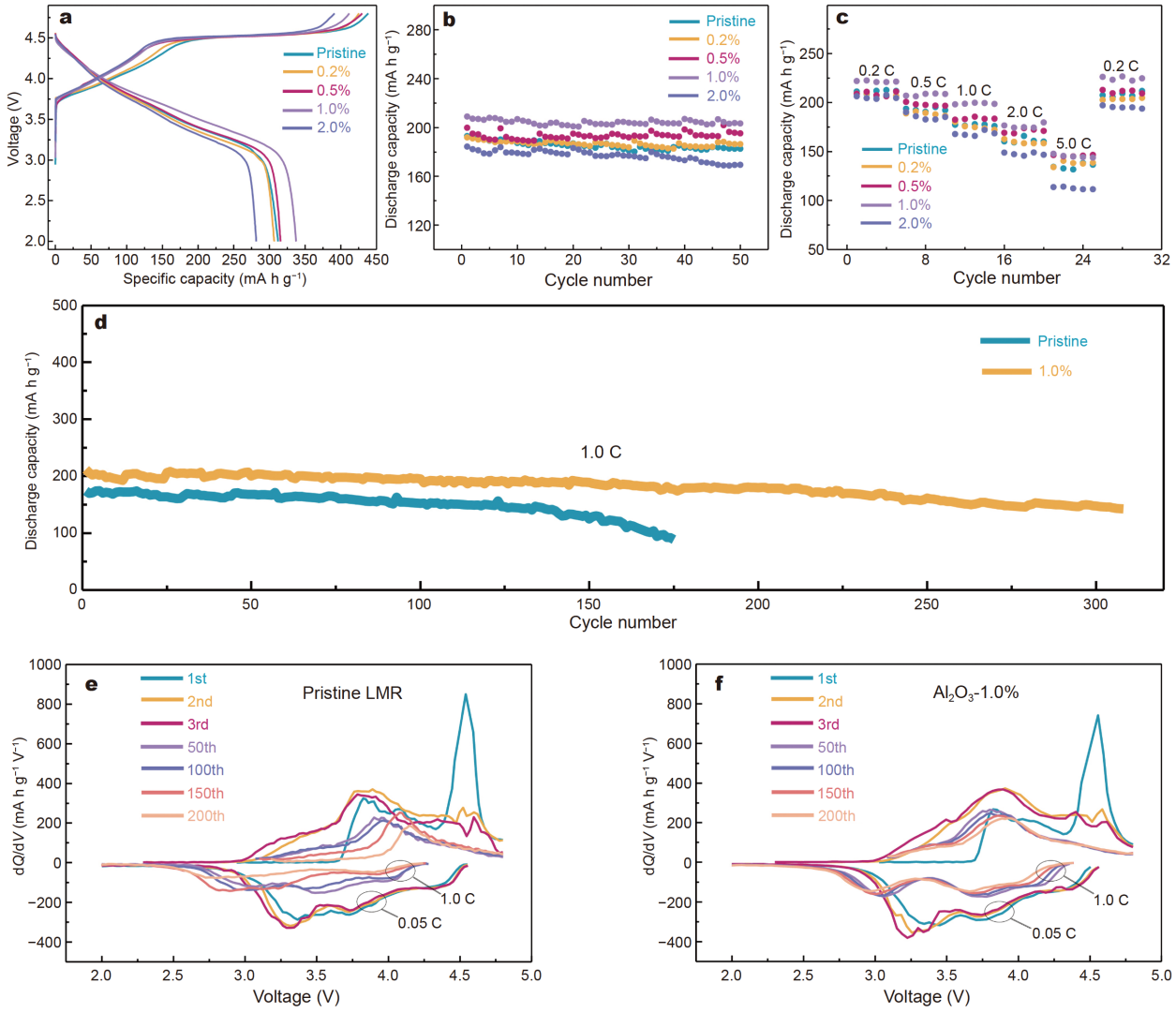

Figure 4 (a) The first charge-discharge voltage curves at the current density of 0.05 C; (b) the cycling performances at the current density of 0.5 C; (c) the rate performances of the pristine LMR material and Al_2O_3-coated LMR; (d) cycling performances of the pristine material and Al_2O_3-1.0% LMR obtained at 1.0 C; the dQ/dV plots of (e) the pristine material and (f) Al_2O_3-1.0% LMR for the charge-discharge curves at different cycles.

Moreover, the cycling behavior was examined at various current densities from 0.2 C up to 5.0 C. As shown in Fig. 4c, the discharge capacities of all samples decrease with increasing rates. The capacity of Al_2O_3-1.0% is significantly higher than that of the pristine LMR at low rates, demonstrating its superior SEI properties. It is most likely that under lower rates the coating minimizes the contact of electrode materials with electrolyte, inhibiting side reactions and reducing SEI thickness during the cycle, thus facilitating facile Li^+ transfer. Nevertheless, at high current densities of 2 and 5 C, the performance of the Al_2O_3-coated LMR was similar to that of the pristine LMR (Fig. 4c) and limited improvement was observed. This suggests that surface modification has minimal effect on the Li^+ diffusion. Given the electrochemical inertness of Al_2O_3, a thicker coating increases the barrier for electron and Li^+ ion conduction, and may explain the poor rate performance of the Al_2O_3-2.0%. In addition, when the current density switches back to 0.2 C, the initial capacities of all samples are recovered, illustrating the modified material has excellent reversibility.

Long-term stability tests were done to evaluate the effectiveness of Al_2O_3-1.0% in practical applications. Cycling was performed on the pristine LMR and Al_2O_3-1.0% LMR at 1.0 C (Fig. 4d). Capacity retention of Al_2O_3-1.0% was as high as 84.9% after 200 cycles, while the pristine

LMR lost 61.4% of its initial capacity after 175 cycles. After 200 cycles for Al_2O_3-1.0%, there is no significant capacity decay. Based on the improvement in electrochemical performances from pristine to the Al_2O_3-coated LMR, Al_2O_3 coating can significantly enhance the cycle stability of the LMR.

Al_2O_3 coating was also applied to the electrochemically unstable NMC622 to test its effectiveness on other types of cathode materials (Fig. S4).

To reiterate, the capacity fade of the Li half-cell is mainly caused by the interface reactions between the electrolyte and cathode and associated with crystal phase transformations. The integrated area of the differential capacity profile for the pristine LMR shows marked decrease after 50 cycles. The myriad parasitic reactions at the surface of cathode materials results in limited Li^+ transport from the electrolyte to cathode (Fig. 4e). After 150 cycles, the Ni^{4+}/Ni^{2+} and Mn^{4+}/Mn^{3+} redox peaks at 3.7 and 3.4 V decrease and a redox peak emerges around 2.6 V, which corresponds to the phase transformation from layered to spinel, and results in a large capacity loss (Fig. 4e). This can also be observed in the cycling data where the capacity drops sharply near the 200th cycle (Fig. 4d). In contrast, with the Al_2O_3 coating, the peak of Ni^{4+}/Ni^{2+} redox remains unchanged even after 200 cycles. The corresponding Mn^{4+}/Mn^{3+} redox still remains above 3.0 V and its intensity is strong (Fig. 4f).

In Fig. 5a, the pristine LMR shows a rapid voltage drop and capacity fade. In comparison, the voltage decay for Al_2O_3-1.0% is significantly ameliorated (Fig. 5b). Fig. 5c presents more clearly that the voltage for the uncoated LMR dropped from 3.6 to 3.15 V with a 12.5% loss after 150 cycles, while the average voltage for the Al_2O_3-1.0% LMR was maintained at nearly 96.3% of its original voltage after cycling under the same conditions. This evinces that the presence of the Al_2O_3 coating effectively enhanced the interfacial stability of the bulk active material. In addition, oxygen evolution on the surface of the cathode material is closely related to the voltage decay [43]. Fig. 5d shows that the exothermic temperature of the Al_2O_3-1.0% LMR is delayed with lower heat generation, and further confirms the interface stability of Al_2O_3-coated LMR.

Impedance spectroscopy was used to understand the effects of Al_2O_3 coating on the initial and post-cycle electrochemical kinetics of the LMR material. Fig. 5e displays the impedance spectra after three cycles. The sizes of the semicircles in the curve are 58.3, 73.4, 76.8 and 110.7 Ω for Al_2O_3-0.2%, Al_2O_3-0.5%, Al_2O_3-1.0%, Al_2O_3-2.0%, respectively, which are greater than those of the pristine materials, mainly due to the insulating nature of Al_2O_3. Although the initial resistance of the Al_2O_3-coated materials is high, it remains unchanged for Al_2O_3-1.0% after 200 cycles while the impendence of the pristine

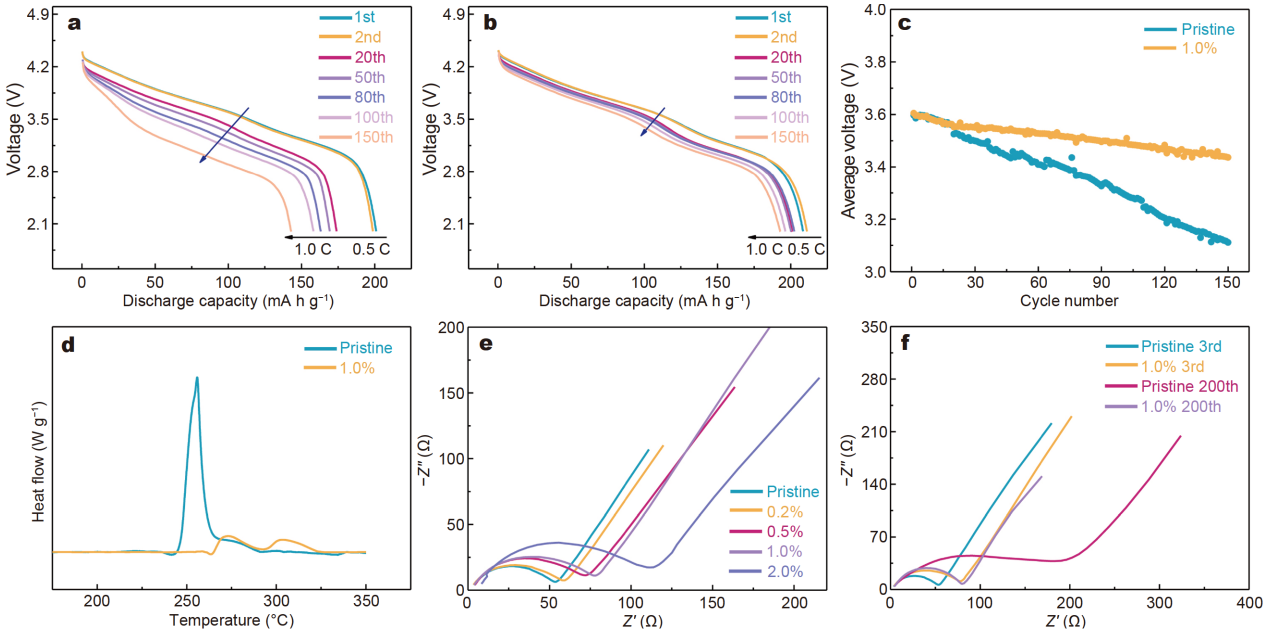

Figure 5 The voltage evolution of the (a) pristine material and (b) Al_2O_3-coated LMR during cycling; (c) the average voltages of the pristine material and Al_2O_3-coated LMR during cycling; (d) the DSC curves of the pristine material and Al_2O_3-1.0% LMR at charged state of 4.8 V; (e) the EIS of the pristine material and Al_2O_3-coated LMR at the 3rd cycle; (f) the EIS of the pristine material and Al_2O_3-1.0% LMR at the 3rd cycle and 200th cycle.

LMR increases steadily from 50.8 to 200.7 Ω (Fig. 5f). This result shows that the Al_2O_3 layer with optimized thickness can effectively limit side reactions, and suppress the gradual increase in interfacial resistance of electrode/electrolyte during cycling. This further demonstrates that the Al_2O_3-1.0% coated LMR possesses excellent interfacial stability and electrochemical properties.

Safety analysis

Safety is one of the most critical aspects for LIBs. Poor thermal stability is the major cause of battery thermal runaway in cases of an internal short circuit. The reactive oxygen molecules generated by electrolyte decomposition react vigorously with the electrolyte to release large amounts of heat and gas. In addition, active oxygen molecules can diffuse to the negative electrode and react violently with the anode material. The pristine material and the Al_2O_3-1.0% were charged to a highly delithiated state at 4.8 V, and the change in thermal behavior was measured by DSC. In this highly delithiated state, the crystal structure of the material is unstable and causes oxygen to be released from the transition metal layer. As shown in Fig. 5d, the exotherm of the pristine material is concentrated near 255°C with a heat release of 555.6 J g^{-1}. The Al_2O_3-1.0% LMR has two smaller exothermic peaks appear near 273 and 303°C with a heat release of only 153.6 J g^{-1}. The results show that the Al_2O_3 coating can suppress side reactions at the surface of LMR and improve thermal stability in cases of overpotential or overcharge states.

CONCLUSIONS

In summary, a commercially available thin-film coating method based on microemulsion is proposed here and used to fabricate layered cathode materials with a uniform metal oxide protective layer at a large-scale. In addition, solvents were recycled and reused for improved environmental and economical considerations. The LMR cathodes coated with Al_2O_3 thin film was presented and studied as an example due to its promise and well-documented poor ICE and capacity fade. By adjusting the Al^{3+} content in the microemulsion, the thickness of the coating could be carefully controlled. The resulting ICE increased from 71.2% to 82.0%. With an Al_2O_3 coating with optimized thickness, the SEI formed on the cathode surface appears to be thin (~8 nm) and stable that increases low-rate performance and improves cycle stability. Moreover, the uniform coating of Al_2O_3 minimizes the contact between the electrolyte and electrode, hindering electrolyte decomposition, as well as reducing oxygen loss, phase transformation, and voltage decay. The energy density of the battery material is maintained, and its safety is largely improved. As a result, capacity retention for LMR 1% reached 84.9% even after 200 cycles at 1.0 C. Thermal stability was also improved. The exothermic peak of the Al_2O_3-1.0% LMR sample in the 4.8 V delithiated state rose from 255 to 273°C with an associated heat release reduced by 72.4%.

Received 2 January 2020; accepted 2 April 2020; published online 11 June 2020

1 Armand M, Tarascon JM. Building better batteries. Nature, 2008, 451: 652–657
2 Feng X, Ouyang M, Liu X, *et al.* Thermal runaway mechanism of lithium ion battery for electric vehicles: a review. Energy Storage Mater, 2018, 10: 246–267
3 Chen X, Li H, Yan Z, *et al.* Structure design and mechanism analysis of silicon anode for lithium-ion batteries. Sci China Mater, 2019, 62: 1515–1536
4 Zhao Y, Kang Y, Wang L, et al. Silicon-based and -related materials for lithium-ion batteries. Prog Chem, 2019, 31: 613–630
5 Shi JL, Xiao DD, Ge M, *et al.* High-capacity cathode material with high voltage for Li-ion batteries. Adv Mater, 2018, 30: 1705575
6 Hu M, Pang X, Zhou Z. Recent progress in high-voltage lithium ion batteries. J Power Sources, 2013, 237: 229–242
7 Li M, Lu J, Chen Z, *et al.* 30 years of lithium-ion batteries. Adv Mater, 2018, 30: 1800561
8 Li W, Song B, Manthiram A. High-voltage positive electrode materials for lithium-ion batteries. Chem Soc Rev, 2017, 46: 3006–3059
9 Manthiram A, Song B, Li W. A perspective on nickel-rich layered oxide cathodes for lithium-ion batteries. Energy Storage Mater, 2017, 6: 125–139
10 Noh HJ, Youn S, Yoon CS, *et al.* Comparison of the structural and electrochemical properties of layered $Li[Ni_xCo_yMn_z]O_2$ (x=1/3, 0.5, 0.6, 0.7, 0.8 and 0.85) cathode material for lithium-ion batteries. J Power Sources, 2013, 233: 121–130
11 Rozier P, Tarascon JM. Review—Li-rich layered oxide cathodes for next-generation Li-ion batteries: chances and challenges. J Electrochem Soc, 2015, 162: A2490–A2499
12 Zhao Q, Guo Z, Wu Y, *et al.* Hierarchical flower-like spinel manganese-based oxide nanosheets for high-performance lithium ion battery. Sci China Mater, 2019, 62: 1385–1392
13 Cai Y, Ku L, Wang L, *et al.* Engineering oxygen vacancies in hierarchically Li-rich layered oxide porous microspheres for high-rate lithium ion battery cathode. Sci China Mater, 2019, 62: 1374–1384
14 Pan H, Zhang S, Chen J, *et al.* Li- and Mn-rich layered oxide cathode materials for lithium-ion batteries: a review from fundamentals to research progress and applications. Mol Syst Des Eng, 2018, 3: 748–803
15 Seo DH, Lee J, Urban A, *et al.* The structural and chemical origin of the oxygen redox activity in layered and cation-disordered Li-excess cathode materials. Nat Chem, 2016, 8: 692–697
16 Rana J, Kloepsch R, Li J, *et al.* On the structural integrity and electrochemical activity of a $0.5Li_2MnO_3{\cdot}0.5LiCoO_2$ cathode material for lithium-ion batteries. J Mater Chem A, 2014, 2: 9099–9110

17 Ding F, Li J, Deng F, *et al.* Surface heterostructure induced by $PrPO_4$ modification in $Li_{1.2}[Mn_{0.54}Ni_{0.13}Co_{0.13}]O_2$ cathode material for high-performance lithium-ion batteries with mitigating voltage decay. ACS Appl Mater Interfaces, 2017, 9: 27936–27945
18 Chen Z, Ren Y, Jansen AN, *et al.* New class of nonaqueous electrolytes for long-life and safe lithium-ion batteries. Nat Commun, 2013, 4: 1513
19 Seo HR, Lee HR, Kang DK, *et al.* Surface-initiated fluoride-scavenging polymeric layer on cathode materials for lithium-ion batteries. J Ind Eng Chem, 2017, 53: 425–428
20 Zhan C, Wu T, Lu J, *et al.* Dissolution, migration, and deposition of transition metal ions in Li-ion batteries exemplified by Mn-based cathodes: a critical review. Energy Environ Sci, 2018, 11: 243–257
21 Hu E, Bak SM, Liu Y, *et al.* Utilizing environmental friendly iron as a substitution element in spinel structured cathode materials for safer high energy lithium-ion batteries. Adv Energy Mater, 2016, 6: 1501662
22 Liu X, Ren D, Hsu H, *et al.* Thermal runaway of lithium-ion batteries without internal short circuit. Joule, 2018, 2: 2047–2064
23 Yu FD, Que LF, Xu CY, *et al.* Dual conductive surface engineering of Li-rich oxides cathode for superior high-energy-density Li-ion batteries. Nano Energy, 2019, 59: 527–536
24 Li C, Zhang HP, Fu LJ, *et al.* Cathode materials modified by surface coating for lithium ion batteries. Electrochim Acta, 2006, 51: 3872–3883
25 Zhang X, Xie X, Yu R, *et al.* Improvement of the cycling stability of Li-rich layered Mn-based oxide cathodes modified by nanoscale $LaPO_4$ coating. ACS Appl Energy Mater, 2019, 2: 3532–3541
26 Ben L, Yu H, Wu Y, *et al.* Ta_2O_5 coating as an HF barrier for improving the electrochemical cycling performance of high-voltage spinel $LiNi_{0.5}Mn_{1.5}O_4$ at elevated temperatures. ACS Appl Energy Mater, 2018, 1: 5589–5598
27 Zhao Y, Lv Z, Xu T, *et al.* SiO_2 coated $Li_{1.2}Ni_{0.2}Mn_{0.6}O_2$ as cathode materials with rate performance, HF scavenging and thermal properties for Li-ion batteries. J Alloys Compd, 2017, 715: 105–111
28 Yang S, Wang P, Wei H, *et al.* $Li_4V_2Mn(PO_4)_4$-stablized $Li[Li_{0.2}Mn_{0.54}Ni_{0.13}Co_{0.13}]O_2$ cathode materials for lithium ion batteries. Nano Energy, 2019, 63: 103889
29 Liu W, Oh P, Liu X, *et al.* Countering voltage decay and capacity fading of lithium-rich cathode material at 60°C by hybrid surface protection layers. Adv Energy Mater, 2015, 5: 1500274
30 Zheng F, Yang C, Xiong X, *et al.* Nanoscale surface modification of lithium-rich layered-oxide composite cathodes for suppressing voltage fade. Angew Chem Int Ed, 2015, 54: 13058–13062
31 Li B, Wang J, Cao Z, *et al.* The role of SnO_2 surface coating in the electrochemical performance of $Li_{1.2}Mn_{0.54}Co_{0.13}Ni_{0.13}O_2$ cathode materials. J Power Sources, 2016, 325: 84–90
32 Zhang S, Gu H, Tang T, *et al. In situ* encapsulation of the nanoscale Er_2O_3 phase to drastically suppress voltage fading and capacity degradation of a Li- and Mn-rich layered oxide cathode for lithium ion batteries. ACS Appl Mater Interfaces, 2017, 9: 33863–33875
33 Zhou Y, Bai P, Tang H, *et al.* Chemical deposition synthesis of desirable high-rate capability Al_2O_3-coated $Li_{1.2}Mn_{0.54}Ni_{0.13}Co_{0.13}O_2$ as a lithium ion battery cathode material. J Electroanal Chem, 2016, 782: 256–263
34 Xu GL, Liu Q, Lau KKS, *et al.* Building ultraconformal protective layers on both secondary and primary particles of layered lithium transition metal oxide cathodes. Nat Energy, 2019, 4: 484–494
35 Meng X, Yang XQ, Sun X. Emerging applications of atomic layer deposition for lithium-ion battery studies. Adv Mater, 2012, 24: 3589–3615
36 Ahn D, Xiao X. Extended lithium titanate cycling potential window with near zero capacity loss. Electrochem Commun, 2011, 13: 796–799
37 Sopha H, Salian GD, Zazpe R, *et al.* ALD Al_2O_3-coated TiO_2 nanotube layers as anodes for lithium-ion batteries. ACS Omega, 2017, 2: 2749–2756
38 Zhang W, Liu Y, Wu J, *et al.* Surface modification of $Li_{1.2}Mn_{0.54}Ni_{0.13}Co_{0.13}O_2$ cathode material with Al_2O_3/SiO_2 composite for lithium-ion batteries. J Electrochem Soc, 2019, 166: A863–A872
39 Li L, Chen Z, Zhang Q, *et al.* A hydrolysis-hydrothermal route for the synthesis of ultrathin $LiAlO_2$-inlaid $LiNi_{0.5}Co_{0.2}Mn_{0.3}O_2$ as a high-performance cathode material for lithium ion batteries. J Mater Chem A, 2015, 3: 894–904
40 Zhang J, Zhang H, Gao R, *et al.* New insights into the modification mechanism of Li-rich $Li_{1.2}Mn_{0.6}Ni_{0.2}O_2$ coated by Li_2ZrO_3. Phys Chem Chem Phys, 2016, 18: 13322–13331
41 Wen X, Liang K, Tian L, *et al.* Al_2O_3 coating on $Li_{1.256}Ni_{0.198}Co_{0.082}Mn_{0.689}O_{2.25}$ with spinel-structure interface layer for superior performance lithium ion batteries. Electrochim Acta, 2018, 260: 549–556
42 Chen Y, Wang X, Zhang J, *et al.* Al_2O_3-coated $Li_{1.2}Mn_{0.54}Ni_{0.13}Co_{0.13}O_2$ nanotubes as cathode materials for high-performance lithium-ion batteries. RSC Adv, 2019, 9: 2172–2179
43 Hu E, Yu X, Lin R, *et al.* Evolution of redox couples in Li- and Mn-rich cathode materials and mitigation of voltage fade by reducing oxygen release. Nat Energy, 2018, 3: 690–698

Acknowledgements This work was supported by the National Natural Science Foundation of China (U1564205), the Project of Construction of Innovative Teams and Teacher Career Development for Universities and Colleges under Beijing Municipality (IDHT20180508). Li T is thankful for the Northern Illinois University startup support.

Author contributions Li J, Li T and Zhao Y conceived and developed the concept. Kang Y, Li J and Zhao Y prepared the materials. Kang Y, Zhao Y, Xu H and Qian K contributed to the experiments. Zhao Y, Kang Y and Li T analyzed the data and wrote the manuscript. Zhao Y, Li J, He X and Liang Z reviewed and edited the manuscript before submission. All authors contributed to the general discussion.

Conflict of interest The authors declare that they have no conflict of interest.

Supplementary information Supporting data are available in the online version of the paper.

Jiangang Li received his BSc degree in chemistry from Shanxi University in 1987. He completed his PhD in the Department of Applied Chemistry at Tianjin University in 2001. Then he carried out his postdoctoral research with Prof. Chunrong Wan in the Institute of Nuclear and New Energy Technology at Tsinghua University in 2002–2004. He worked as a visiting scholar with Prof. Guozhong Cao at the University of Washington in 2009–2010. He is currently a professor in the School of Chemical Engineering at Beijing Institute of Petrochemical Technology. His current research interests focus on the advanced materials for energy conversion and storage such as batteries and supercapacitors.

Tao Li earned his BSc degree in polymer material science and engineering from the East China University of Science and Technology in 2003. He completed his PhD in the Department of Chemistry and Biochemistry at the University of South Carolina—Columbia in 2009. He is currently an assistant professor in the Department of Chemistry and Biochemistry at Northern Illinois University and holds a joint scientist position at the Advanced Photon Source at Argonne National Lab. His research interests focus on using advanced X-ray techniques to study the self-assembly of nanoparticles as well as energy materials including catalyst and battery.

大规模制备氧化铝均匀包覆的富锂锰基正极材料用于锂离子电池

亢玉琼[1,2†], 梁正[5†], 赵云[3,4*], 徐海平[4], 钱坤[4], 何向明[3], 李涛[4*], 李建刚[1,2*]

摘要 因其高容量、高电压和低成本的特点，富锂锰基氧化物(LMR)作为锂离子电池(LIB)正极材料具有广阔的应用前景. 然而, 其较低的首次库仑效率(ICE)和不稳定的电极/电解质界面, 使电池阻抗较高和电压衰减较快, 从而导致电池出现较快的容量损失并引发安全问题. 在这项工作中, 我们通过微乳液法在LMR正极材料表面均匀涂覆一层氧化铝(Al_2O_3), 以稳定其界面性质. 这种基于微乳液的包覆方法环境友好、成本低, 并且可以大规模应用. 厚度为8 nm的Al_2O_3包覆层可有效稳定LMR电极/电解质界面(ICE提高至82.0%, 并在200圈循环内有效稳定电池阻抗). 此外, 对LMR界面的改性抑制了材料从层状到尖晶石的相变(200圈循环后放电中值电压保持率为96.3%), 并且提升了材料的热稳定性(热量释放减少了72.4%). 总之, 这项研究为解决锂离子电池正极材料的界面问题开辟了一条新途径.